Available online at www.sciencedirect.com
SCIENCE DIRECT®
Biochemical Pharmacology 69 (2005) 147–157
Biochemical Pharmacology
www.elsevier.com/locate/biochempharm

BCL-xL overexpression effectively protects against tetrafluoroethylcysteine-induced intramitochondrial damage and cell death

Han K. Ho[a,*], Zhong-Hua Hu[a,1], Shie-Pon Tzung[b,2], David M. Hockenbery[b], Nelson Fausto[c], Sidney D. Nelson[a], Sam A. Bruschi[a]

[a]*Department of Medicinal Chemistry, University of Washington, Box 357610, Seattle, WA 98195, USA*
[b]*Division of Clinical Research, Fred Hutchinson Cancer Research Center, Seattle, WA 98109, USA*
[c]*Department of Pathology, University of Washington, Seattle, WA 98195, USA*

Received 1 July 2004; accepted 27 August 2004

Abstract

S-(1,1,2,2-Tetrafluoroethyl)-L-cysteine (TFEC), a major metabolite of the industrial gas tetrafluoroethylene, has been shown to mediate nephrotoxicity by necrosis. TFEC-induced cell death is associated with an early covalent modification of specific intramitochondrial proteins; including aconitase, α-ketoglutarate dehydrogenase (KGDH) subunits, HSP60 and HSP70. Previous studies have indicated that the TAMH line accurately models TFEC-induced in vivo cell death with dose- and time-dependent inhibitions of both KGDH and aconitase activities. Here, we show that the molecular pathway leading to TFEC-mediated cell death is associated with an early cytosolic to mitochondrial translocation of BAX, a pro-apoptotic member of the BCL-2 family. Immunoblot analyses indicated movement of BAX (21 kDa) to the mitochondrial fraction after exposure to a cytotoxic concentration of TFEC (250 μM). Subsequent cytochrome *c* release from mitochondria was also demonstrated, but only a modest increase in caspase activities was observed, suggesting a degeneration of early apoptotic signals into secondary necrosis. Significantly, TAMH cells overexpressing BCL-xL preserved cell viability even to supratoxicological concentrations of TFEC (≤600 μM), and this cytoprotection was associated with decreased HSP70i upregulation, indicating suppression of TFEC-induced proteotoxicity. Hence, TFEC-induced necrotic cell death in the TAMH cell line is mediated by BAX and antagonized by the anti-apoptotic BCL-2 family member, BCL-xL.

Keywords: TFEC; BAX translocation; BCL-xL; Cytotoxicity; Intramitochondrial damage; Necrosis

1. Introduction

Mitochondria are increasingly recognized as important targets in drug-induced tissue injury [1]. For example, mitochondrial dysfunction can have a significant impact on overall cell survival if critical intramitochondrial functions of cellular respiration through the TCA cycle and/or the electron transport chain are perturbed. Many groups have also shown that important proteins related to the control of apoptosis (e.g., apoptosis-inducing factor or AIF, cytochrome *c*, and SMAC/DIABLO) are found within this organelle. Release of these proteins, and other essential cell-death signaling components, is now acknowledged to alter cellular viability and organ stasis [2].

Tetrafluoroethylene is an industrial gas used widely as a precursor for Teflon™ coating. It is representative of a broader class of commercially important halogenated aliphatic gases. A major metabolite, tetrafluoroethylcysteine (TFEC), is known to cause both kidney and liver

Abbreviations: AMC, 7-amino-4-methylcoumarin; ATF3, activating transcription factor-3; BSS, buffered saline solution; CHAPS, 3-[(3-cholamidopropyl)dimethylammonio]-1-propanesulfonate; FBS, fetal bovine serum; GAPDH, glyceraldehyde 3-phosphate dehydrogenase; HSP, heat shock protein; INT, iodonitrotetrazolium chloride; KGDH, α-ketoglutarate dehydrogenase; MTT, 3-(4,5-dimethylthiazol-2-yl)-2,5-diphenyl-tetrazolium bromide; PIPES, piperazine-N,N′-bis(2-ethanesulfonic acid); TNF, tumor necrosis factor; VDAC, voltage-dependent anion-selective channel

* Corresponding author. Tel.: +1 206 543 8503; fax: +1 206 685 3252.
E-mail address: hankiat@u.washington.edu (H.K. Ho).
[1] Present address: Amgen Inc., Seattle, WA 98119, USA.
[2] Present address: Harborview Medical Center, Seattle, WA 98104, USA.

0006-2952/$ – see front matter © 2004 Elsevier Inc. All rights reserved.
doi:10.1016/j.bcp.2004.08.030

damage [3,4]. Ubiquitous aminotransferase activities are considered to mediate β-lyase bioactivation of TFEC, and the most important of these is likely to be the mitochondrial isoform of aspartate aminotransferase [4,5]. Previously, we have investigated the molecular basis of TFEC-induced renal damage and cytotoxicity, and have determined that TFEC-induced nephrotoxicity is associated with the covalent modification of a relatively small set of intra-mitochondrial proteins in vivo, namely, HSP70, HSP60, aspartate aminotransferase, aconitase and the E2/E3 subunits of KGDH [5–7]. These specific protein modifications likely trigger a cascade of mitochondrial and cellular alterations, which eventually results in cell and tissue damage. Although the precise sequence of these events is still not known, the available literature indicates that TFEC induces cell killing exclusively by necrosis with little or no oxidative stress [5,8–10].

Previously, we characterized biochemical changes following TFEC exposure in vitro using a TGFα-overexpressing, mouse hepatocyte cell line (TAMH) and observed dose- and time-dependent inhibitions of both aconitase and KGDH protein target activities which closely resembled comparable mitochondrial deficits in these enzymes in vivo [5,11]. As a result, although the TAMH cell line is not of renal origin, TFEC causes slight hepatotoxicity [3], and the liver-derived TAMH line contains sufficient TFEC bioactivation capability to faithfully reproduce important aspects of the in vivo toxicity of TFEC at toxicologically relevant doses [3,5,12,13].

In the current study, we have extended these observations by examining and modulating TFEC-mediated alterations to pro-apoptotic BAX subcellular localization. Specifically, BAX subcellular translocation was determined in stable transfectants of the parental TAMH cell line either overexpressing the BAX dimerization partner, BCL-xL (TAMH-BCL-xL) or, alternatively, an empty vector control (TAMH-Vc) [14,15]. Since BCL-xL represents the predominant anti-apoptotic BCL-2 family member observed in mouse hepatocytes, these stable lines are most suited to examine BAX translocation following TFEC treatment [15]. Results of studies showed that after TFEC treatment, BAX movement to mitochondria was also accompanied by the release of cytochrome *c* into the cytosol. BCL-xL overexpression was shown to effectively suppress these events and protect against TFEC-induced cellular toxicity.

Our findings are consistent with a role for the BCL-2 family of proteins in ''necrotic'' cell death induced by TFEC, and possibly, extend the well-characterized and pivotal role(s) for the BCL-2 family of proteins in apoptosis [16]. Furthermore, our observations that BCL-xL overexpression reduces TFEC-induced cytotoxicity—as monitored by expression of the ubiquitous heat shock protein HSP70i—is of drug safety and clinical toxicological interest.

2. Materials and methods

2.1. Cell culture

Serum-free cell culture of the TAMH line between passages 21 and 35 was undertaken as previously described [11,13]. Details regarding the stable TAMH-BCL-xL cell line have been previously reported [17]. All chemicals were obtained from Sigma unless otherwise stated. Briefly, cells were grown in serum free Dulbecco's modified Eagle's medium/Ham's F12 (Gibco) supplemented with 5 μg/mL insulin, 5 μg/mL transferrin, 5 ng/mL selenium (Collaborative Biomedical Products), 100 nM dexamethasone, 10 mM nicotinamide and 0.1% (v/v) gentamicin (Gibco). Maintenance of the stable transfectant TAMH-BCL-xL line and the null vector control, TAMH-Vc, were with the additional supplementation of 400 μg/mL G418 sulfate (Gibco). Cultures were maintained in a humidified incubator with 5% carbon dioxide/95% air at 37 °C and passaged at 70–90% confluence.

2.2. Dosing and harvesting of cells

Cultures were treated at approximately 80% confluence by replacement of growth medium with fresh medium containing 250 μM of freely soluble TFEC. To provide sufficient material for immunoblot assays, TAMH-Vc or TAMH-BCL-xL cultures were grown in larger 150 cm^2 tissue culture flasks (cf. 25 or 75 cm^2). During harvesting, medium was aspirated and cells washed twice with ice-cold PBS. 200 μL of lysis buffer (20 mM Tris, 0.25 mM sucrose, 1 μM DTT, protease inhibitor cocktail (Roche)) was added to each dish. Cells were scraped off using a rubber policeman and kept at 0 °C prior to generation of whole-cell lysates by sonication with an ultrasonic probe tip (Series 4710, Cole-Palmer). For immunoblots examining BAX translocation and cytochrome *c* release, isolation of TAMH-Vc or TAMH-BCL-xL subcellular fractions was carried out prior to sonication as detailed below.

2.3. Subcellular fraction isolation

Mitochondria-enriched fractions were isolated with slight modifications to the protocol described previously [18]. Briefly, the harvested cells were spun using a bench top microcentrifuge to form a pellet. Supernatant was removed and the pellet was lysed in 100 μL (per million cells) of digitonin lysis buffer (75 mM NaCl, 1 mM NaH_2PO_4, 8 mM Na_2HPO_4, 250 mM sucrose, 200 μg/mL digitonin, and protease inhibitor cocktail) with gentle but thorough resuspension for 10 min. The lysate was centrifuged at 13,000 × *g* for 5 min at 4 °C. The resultant supernatant was collected as the cytosolic fraction. The pellet was then resuspended with a fresh volume of digitonin lysis buffer, sonicated for 5 s and centrifuged at 13,000 × *g* for 5 min at 4 °C. The supernatant contained

the mitochondria-enriched fraction. The efficiency of subcellular fractionations was confirmed by immunoblotting with antisera to mitochondrially-located VDAC or cytosolic GAPDH as described below.

2.4. Immunoblotting

All the fractions collected were assayed for protein concentration using the BCA protein assay kit (Pierce). Sample proteins (30–50 μg) were resolved by denaturing electrophoresis using 15% SDS–PAGE (Mini-PROTEAN II, Bio-Rad Laboratories) and transferred to nitrocellulose membrane for 1 h at 15 V using Trans-Blot SD Semi-Dry Transfer Cell (Bio-Rad). Immunodetection was by chemiluminescence (SuperSignal ULTRA, Pierce) using specific antibodies diluted in PBS with 0.05% (v/v) Tween 20 and 5% (w/v) powdered milk. Anti-ATF3, anti-VDAC and anti-BCL-xL were from Santa Cruz Biotechnology; anti-HSP70i (1:1000) from Stressgen; anti-BAX and anti-cytochrome *c* from Pharmingen and anti-GAPDH (1:2500) was made in-house [19]. Secondary anti-mouse and anti-rabbit horseradish peroxidase conjugated secondary antibodies (Pierce) were used at 1:20,000 dilution. All antibodies were used at 1:2000 dilution unless otherwise stated.

2.5. Densitometric analysis

Nitrocellulose membranes and X-ray films were analyzed after immunoblotting using Bio-Rad ChemiDoc and Quantity One Version 4.3.0 program (Bio-Rad). The bands were cropped and their intensities were quantified. Film exposure was from 1 to 10 min depending on signal intensity.

2.6. Immunocytochemistry

Cells were grown on 2 and 4-well chambered slides (Labtek II, Nalgen). Cultures were dosed as described above. After treatment, medium was aspirated and cells were stained with 500 nM MitoTracker™ Red (Molecular Probes) for 20 min, washed twice with Hank's BSS and fixed with 3.7% (v/v) paraformaldehyde (EMS) in Hank's BSS for 20 min at RT. Ice-cold acetone was added and the mixture was allowed to stand for 5 min to permeabilize the plasma membrane and non-specific binding was blocked by soaking the chambers overnight in PBS with 10% FBS at 4 °C. Immunostaining was with anti-BAX (Pharmingen) and Alexa-Fluor 488-conjugated anti-mouse IgG (Molecular Probes) for 2 h incubation each (dilutions between 1:50 and 1:200). Saponin (0.2%, w/v) was added with the immunostaining reagents to enhance antibody accessibility. Slides were mounted with Fluoromount G (Southern Biotechnologies) and examined using a Nikon Diaphot 200 fluorescent microscope (Nikon) with 40× magnification. The images were captured with Princeton Instruments MicroMax CCD (Universal Imaging).

2.7. Viability assay by MTT

Cells were seeded and grown to confluence on 96-well plates (approximately 10,000 cells in each well). After TFEC treatment, 50 μL MTT dye (2.5 mg/mL in PBS) was added per well with another 200 μL HEPES-buffered growth medium and incubated at 37 °C in the dark for 4 h. The dye was then aspirated and 25 μL of Sorenson's buffer (0.1 M glycine, 0.1 M NaCl equilibrated to pH 10.5 with 0.1 M NaOH) and 200 μL of dimethyl sulfoxide were added immediately to each well. The plates were read at 560 nm using a microtiter plate reader (Molecular Devices) as previously described [20].

2.8. Cytotoxicity assay by LDH release

LDH release was determined quantitatively using microtiter plate modifications of standard iodonitrotetrazolium chloride (INT)-coupled colorimetric methods [21]. Briefly, cells grown on 96-well plates were subjected to respective TFEC doses made up in 100 μL of growth medium. At the end of treatment, 20 μL of freshly prepared lactate solution (36 mg/mL in Tris–Cl 10 mM, pH 8.5), 20 μL of INT solution (2 mg/mL in PBS) and 20 μL of NAD^+ solution (3 mg/mL with 13.5 U/mL of diaphorase in PBS containing 0.03% BSA and 1.2% sucrose) was added to each well. The mixture was incubated for 10–30 min at ambient temperature with periodic shaking of the plate. Reactions were quenched with a solution of sodium amino-oxoacetic acid (16.6 mg/mL in PBS). The plates were read at 490 nm on a microtiter plate reader. The data were converted into an arbitrary unit of absorbance/time (per min) before they were expressed as a ratio of non-treated control. Standard deviations were also calculated based on $n = 8$.

2.9. Caspase activation assays

Caspase activation was determined by incubating 30–60 μg of homogenized cell lysates at 37 °C in 100 μL of caspase assay buffer (50 mM PIPES, pH 7.4, 100 mM NaCl, 1 mM EDTA, 10% (w/v) sucrose, 0.1% (w/v) CHAPS, 10 mM DTT) with 20 μM fluorogenic caspase substrates: Ac-DEVD-AMC, Ac-VDVAD-AMC, Ac-VEID-AMC, Ac-IETD-AMC, LEHD-AMC (Alexis Biochemicals) and fluorescence monitored on a Packard Fluorocount (Packard Instrument Company) microplate fluorometer with an excitation wavelength of 360 nm and an emission of 460 nm. Data are presented as *p*mol of AMC hydrolyzed/μg lysate protein/microtiter plate incubation time. The levels of activation were compared

against a positive control treated with 200 nM actinomycin-D and 5 ng/mL TNFα for 8 h (TNFα was added 1 h after addition of actinomycin-D).

2.10. Calpain activation assays

Calpain activation was determined using the same methodology as described for caspases with slight modifications. Briefly, 30–60 μg of homogenized cell lysates were incubated at 37 °C in 100 μL of caspase assay buffer (see above) with 20 μM fluorogenic calpain substrate, Suc-LLVY-AMC (Alexis). Fluorescence from the hydrolyzed products was determined similarly on the plate reader. Data are presented as *p*mol of AMC hydrolyzed/μg lysate protein/microtiter plate incubation time. The specificity of activation was determined by inhibiting the hydrolysis using calpain inhibitors, 100 μM of the peptides ALLM or ALLN (Boehringer Mannheim), made from a 10 mM stock in DMSO.

3. Results

3.1. Effect of TFEC on BAX cytosolic and mitochondrial localization

Immunoblot analyses of TAMH cultures treated with TFEC (250 μM, 0–8 h) revealed a shift in a 21 kDa immunoreactive BAX species from the cytosol to mitochondria at 4 and 8 h post-treatment (Fig. 1A). Although, we observed some BAX localization to mitochondria in the control samples, there was nonetheless a prominent increase in BAX-specific band intensity and mitochondrial translocation with TFEC treatment. In particular, TFEC-specific increases were much more pronounced in the null vector line (TAMH-Vc) in comparison to the TAMH line stably overexpressing BCL-xL (TAMH-BCL-xL; Fig. 1A cf. and B). In addition, densitometric analyses confirmed that TAMH-BCL-xL cultures overexpressed BCL-xL at approximately 8-fold higher levels in comparison to the null vector line (Fig. 1C and D). Consistent with previous reports, we also observed an approximately 60 kDa BAX-immunoreactive species that matches previously reported BAX oligomerization products [22,23] (data not presented). The exact composition of any BAX oligomers has yet to be determined.

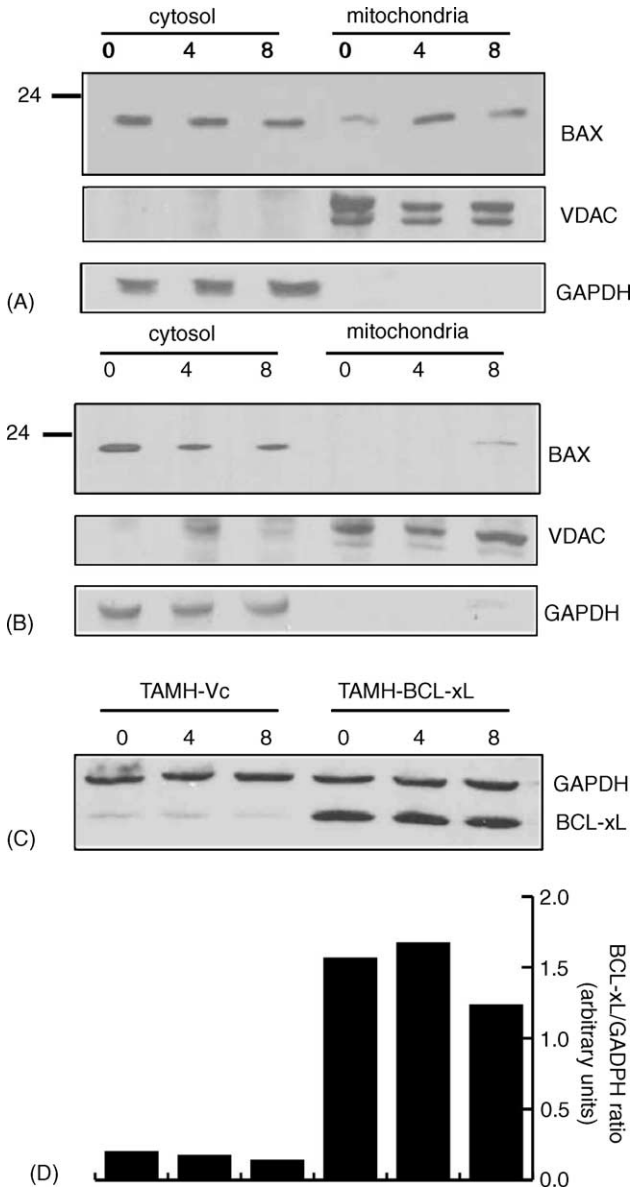

Fig. 1. Immunoblot assay for BAX following TFEC treatment of TAMH-Vc and TAMH-BCL-xL cells. (A) TAMH-Vc cells were treated with 250 μM TFEC for 0, 4 and 8 h. Subcellular fractions of cytosol and mitochondria were separated and immunoblotted with monoclonal α-BAX. Polyclonal α-GAPDH and α-VDAC were employed as loading controls for cytosol and mitochondria, respectively. (B) TAMH-BCL-xL cells were treated and immunoblotted in the same manner as for TAMH-Vc cells above. (C) Total cell lysates from TAMH-Vc and TAMH-BCL-xL cells treated with 250 μM of TFEC for 0, 4 and 8 h immunoblotted with polyclonal α-BCL-xL to confirm the extent of its overexpression in TAMH-BCL-xL cells as compared to TAMH-Vc cells. (D) Densitometric analysis of BCL-xL expression in TAMH-Vc and TAMH-BCL-xL cells, displayed as a ratio of BCL-xL to GAPDH for each treatment time point.

3.2. Immunocytochemical determination of BAX translocation in TAMH-Vc and TAMH-BCL-xL cultures

Independent confirmation of immunoblot assays for BAX intracellular movements in vitro following TFEC treatments was by immunocytochemistry (Fig. 2). Mitotracker™ Red was used as a mitochondrial specific marker and BAX was localized by immunostaining with polyclonal anti-BAX primary antibodies and AlexaFluor 488-conjugated secondary antibodies (refer Section 2.6). Punctate red staining of mitochondria was evident from 2 to 6 h of TFEC treatment of TAMH-Vc cultures, which transformed to an orange coloration (merging of AlexaFluor 488 and Mitotracker™ Red staining). Merged staining was at its most intense in 2 h treated cultures (Fig. 2; left panels) with FITC-immunostained cytosolic

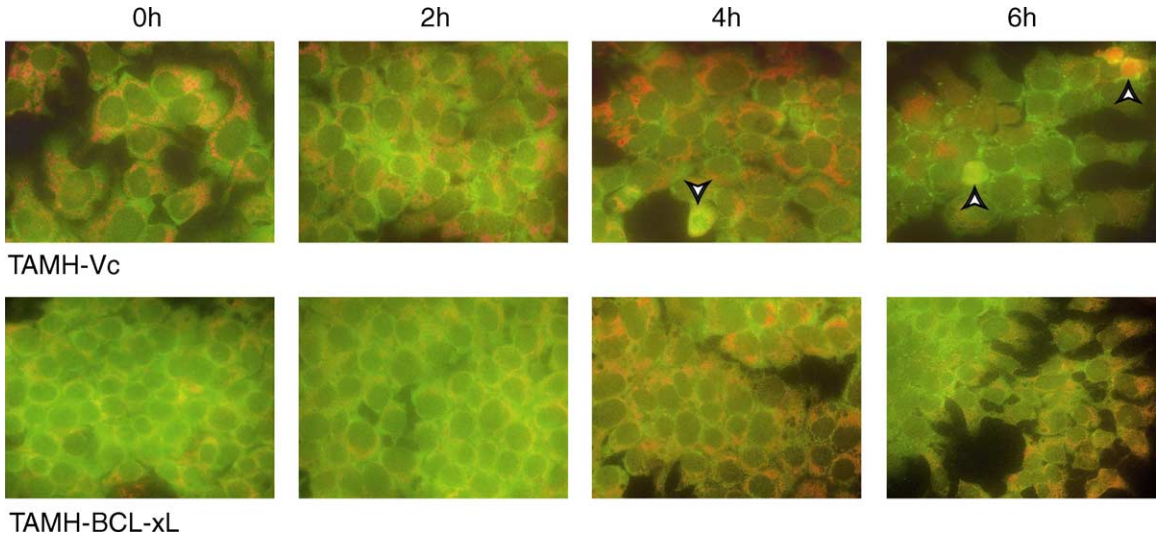

Fig. 2. Immunocytochemical detection of BAX localization. TAMH-Vc (left panel) and TAMH-BCL-xL cells were treated with 250 μM TFEC for 2, 4 and 6 h. Mitochondria were stained with MitoTracker™ Red and BAX with Alexa-Fluor 488-conjugated anti-mouse antibodies. The cells were fixed on a slide and viewed with a fluorescent microscope. Movement of BAX from the cytosol to mitochondria was observed with a progressive decrease in green and corresponding increases in orange/yellow—indicative of dye merging between FITC and MitoTracker™ Red (arrows indicate cells having advanced necrotic morphology).

BAX simultaneously reduced in intensity. Vanishing green and increased colocalization of Mitotracker™ Red and BAX staining (orange merged image) clearly demonstrated that BAX translocated to mitochondria during the course of TFEC treatment in TAMH-Vc cultures, thereby, validating the immunoblot data of Fig. 1. Additionally, we also detected a small fraction of BAX in the mitochondria of 0 h samples (Fig. 2) suggesting that a minor proportion of the total BAX population is constitutively located on the mitochondrial membrane and consistent with the immunoblot data of Fig. 1. In addition, later stage TFEC-treated cultures appeared preferentially altered with respect to morphology and were comparatively low in confluence indicating a loss of cellular adhesion during the progression of TFEC-induced cellular injury (Fig. 2; 4 and 6 h panels of TAMH-Vc).

In comparison, TAMH-BCL-xL cultures displayed little overt morphological changes from 2 to 6 h of TFEC treatment (Fig. 2; lower right panels). Qualitatively, AlexaFluor 488 labeling (i.e., green fluorescence) and cytosolic BAX localization remained almost as intense throughout the course of TFEC exposure in TAMH-BCL-xL overexpressing cultures, suggestive of a failure to activate cytosolic BAX and translocate to mitochondria.

3.3. Cytochrome c release following BAX translocation

Cytochrome *c* release was also examined by Western blot assay. Our observations indicated that cytochrome *c*, which was previously localized exclusively within mitochondria, was released into the cytosol by 8 h with TFEC treatment of the TAMH-Vc cells (Fig. 3A). These data support a well-established model in apoptosis of early BAX translocation to the mitochondria followed by subsequent cytochrome *c* movement into the cytosol. On the other hand, TAMH-BCL-xL cultures did not display significant changes in the mitochondrial localization of cytochrome *c* for up to 8 h of TFEC treatment. Thus, the release

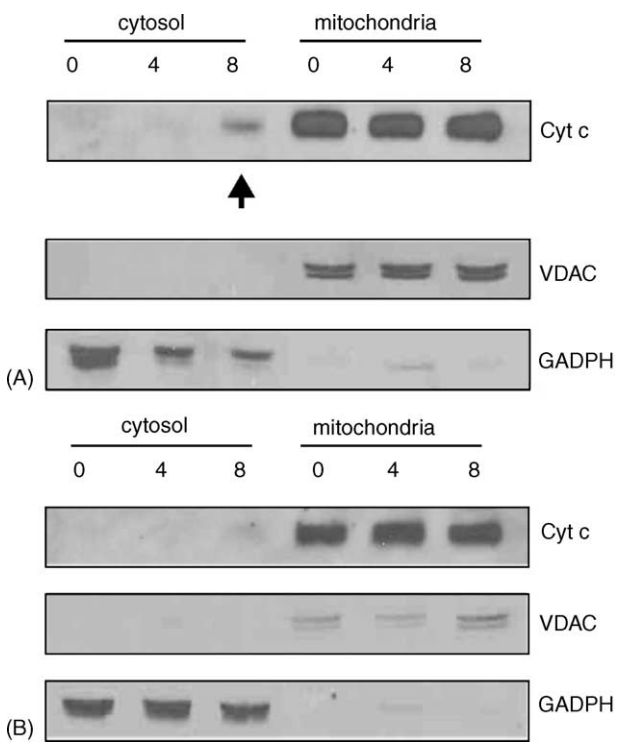

Fig. 3. Immunoblot assay for cytochrome *c* release following TFEC treatment of TAMH-Vc and TAMH-BCL-xL cells. (A) TAMH-Vc cells were treated with 250 μM TFEC for 0, 4 and 8 h. Subcellular fractions of cytosol and mitochondria were separated and immunoblotted with monoclonal α-cytochrome *c*. Polyclonal α-GAPDH and α-VDAC were employed as loading controls for cytosol and mitochondria, respectively. (B) TAMH-BCL-xL cells were treated and immunoblotted in the same manner as for TAMH-Vc cells above (arrow indicates a significant release of cytochrome *c* into the cytosol of TFEC treated TAMH-Vc cells).

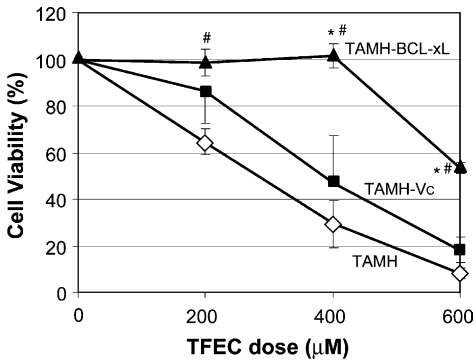

Fig. 4. Viability of TFEC-treated TAMH, TAMH-Vc and TAMH-BCL-xL cells: cells were treated with 200, 400 or 600 μM TFEC for 12 h in total. Viability was measured by MTT assay. Results are expressed as a percentage of viable cells in the untreated controls with ±S.E.M. (* indicates a statistically significant difference between the TAMH-BCL-xL and TAMH-Vc cells, and # indicates a statistically significant difference between TAMH-BCL-xL and TAMH cells as determined by unpaired *t*-test, $P < 0.05$).

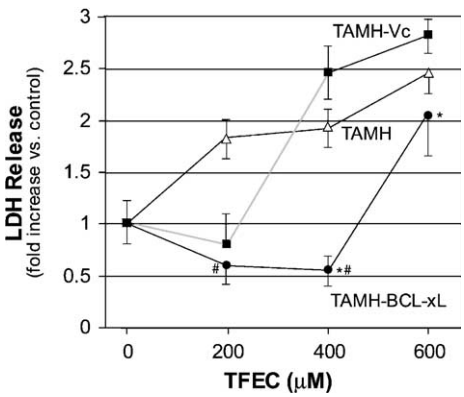

Fig. 5. Cytotoxicity of TFEC-treated TAMH, TAMH-Vc and TAMH-BCL-xL cells: cells were treated with 200, 400 or 600 μM of TFEC for 8 h in total. Cytotoxicity was measured by the cumulative release of LDH into the culture media. Results are expressed as the number of fold increase in LDH activity ($n = 8$) vs. untreated cells (number of fold activity = 1). (* indicates a statistically significant difference between the TAMH-BCL-xL and TAMH-Vc cells, and # indicates a statistically significant difference between TAMH-BCL-xL and TAMH cells, as determined by unpaired *t*-test, $P < 0.05$).

of cytochrome *c* appears impeded in TAMH-BCL-xL cells despite an identical TFEC treatment regimen (Fig. 3B). An apparent time-dependent loss of GADPH was observed in TAMH-Vc cells (Fig. 3A) and this is assumed to be a result of cell lysis due to TFEC treatment since there was no comparable loss of GADPH in TAMH-BCL-xL cells after the same treatment with TFEC (Fig. 3B).

3.4. Inhibition of cell death with BCL-xL overexpression

Stable transfectant TAMH-Vc and TAMH-BCL-xL lines were compared to the parental TAMH line for sensitivities to TFEC-induced toxicities by means of cell viability and cytotoxicity assays. We used the MTT assay to determine the late end-point 24 h survival of cells following continuous TFEC exposure (0–600 μM). An additional advantage for the assessment of cell viability using MTT vital dye was that active mitochondrial enzymes are known to be required to produce the violet color ultimately quantified at 560 nm. BCL-xL overexpression was observed to significantly maintain cell viability with remarkable cytoprotection evident even to very high and toxicologically irrelevant TFEC concentrations (400–600 μM; Fig. 4). For example, at 600 μM TFEC the cellular viability was still about 55% at this late time. On the other hand, TAMH-Vc and parental TAMH lines showed progressive cell killing from below 200 to 600 μM. Near complete cytotoxicity was observed at 600 μM TFEC in the non-BCL-xL overexpressing lines with viability measured at approximately 20% and 10% (Fig. 4). Arguably, MTT viability is reliant on an active mitochondrial respiration and our results may have been confounded by TFEC-mediated mitochondrial dysfunction. Thus, an alternative measure of toxicity was employed in order to corroborate the MTT data.

Complementary results were obtained for cytotoxicity measured as a function of intracellular LDH released into the culture medium due to plasma membrane rupture (Fig. 5). This assay was performed at 8 h after TFEC treatment in order to avoid the confounding effects of protease digestion of released LDH, which contributes to a short half-life in the culture medium (approximately 9 h in the medium[1]). Consistent with the MTT data, both parental TAMH and TAMH-Vc cultures showed proportional increase in LDH release, which doubled at 200–400 μM TFEC concentrations. In contrast, BCL-xL overexpression kept LDH release to a basal level for TFEC concentrations up to 400 μM (Fig. 5). However, a lack of concordance between the MTT and LDH release data at 600 μM TFEC was evident with an apparent convergence of cytotoxicity in all 3 cell lines using LDH release criteria. A likely explanation for this discrepancy is that inhibition of mitochondrial function by TFEC accentuates the differences between BCL-xL overexpressed and control cell lines using the MTT assay, especially when the assay is performed after a long period of incubation (i.e, 24 h). Nonetheless, BCL-xL effectively blocked cell death induced by toxicologically very high concentrations of TFEC using two independent criteria of assessment.

3.5. BCL-xL mediated prevention of TFEC-induced proteotoxicity

The impact of BCL-xL overexpression on other molecular determinants of cellular survival was also examined. Induction of cytosolic HSP70i represents a robust marker for cellular stress and protein damage [24]. In addition,

[1] Information taken from Promega Technical Bulletin No. 306, Version 5/03.

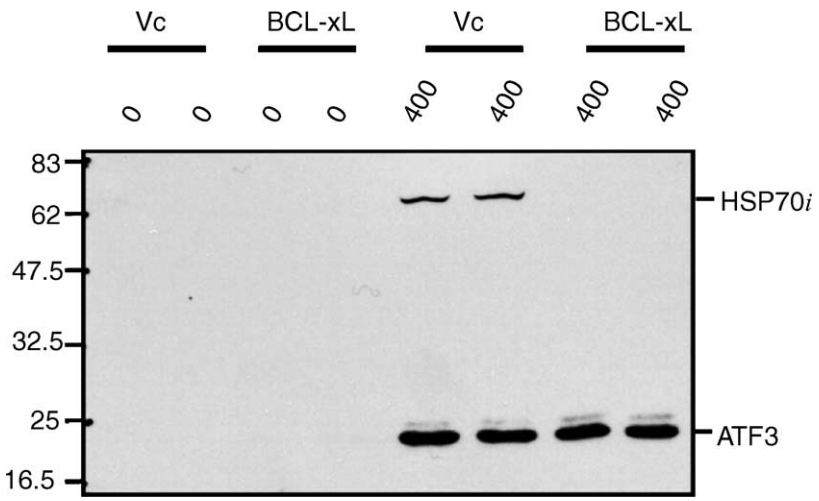

Fig. 6. Effects of TFEC treatment on HSP70i and ATF3 expression: TAMH-Vc and TAMH-BCL-xL cells were treated with TFEC (400 μM) for 4 h followed by incubation in standard growth medium not containing TFEC for a further 8 h (12 h in total). Immunoblot assays were performed using 20 μg total cell lysate protein loaded onto each lane and blotted with polyclonal α-ATF3 and monoclonal α-HSP70i.

activating transcription factor-3 (ATF3) has also been established as a highly stress-inducible transcriptional repressor to numerous chemicals and stressors in mammalian systems [13,25,26]. The levels of expression of HSP70i and ATF3 were examined by immunoblot in both TAMH-BCL-xL and TAMH-Vc lines in a pulse/chase experiment (Fig. 6). Cultures were exposed to vehicle or TFEC (400 μM) for 4 h and then allowed to recover in the presence of fresh growth medium for an additional 8 h (i.e., total time of 12 h) prior to preparation of cell lysates and subsequent analysis. ATF3 was observed to be strongly induced only with TFEC treatment (Fig. 6; right lanes). Interestingly, the expression level of ATF3 was similar for both TFEC-treated TAMH-BCL-xL and TAMH-Vc cell lines. HSP70i levels were also strongly upregulated with TFEC exposure but only in TAMH-Vc cultures (Fig. 6). In comparison, neither ATF3 nor HSP70i could be detected in TAMH-BCL-xL and TAMH-Vc cultures in the absence of added TFEC (Fig. 6, left lanes). Hence, BCL-xL overexpression suppressed TFEC-mediated increases in HSP70i expression in this cell line.

3.6. Caspase activity assays

Based on our observations of early mitochondrial changes, BAX translocations and cytochrome *c* release we also examined the contribution of various caspase activities in the mechanism of TFEC-mediated TAMH cell killing. Caspases are known as downstream effectors of ''classical'' apoptosis in response to the release of cytochrome *c* and apoptosome formation in the cytosol. Five key caspases, including the ''initiators'' (caspase-2, -8 and -9) and the ''executioners'' (caspase-3/7, -6) were investigated using hydrolysis of directed tetrapeptide/pentapeptide fluorogenic substrates (Fig. 7). For all of the caspase activities studied, only modest activation (at most, 10% of positive control levels) were observed with TFEC-treatment at any of the time points examined (Fig. 7). Caspase 3/7 activities in BCL-xL overexpressing cell line were even below detection limits. Furthermore, activities generally appeared diminished in TAMH-BCL-xL versus TAMH-Vc or TAMH lines (Fig. 7). However, these levels of activity were minor in comparison to TNFα/actinomycin-D treated apoptosis positive controls dosed over the same duration (i.e., 8 h; Fig. 7).

3.7. Calpain activity assays

The lack of significant caspase activation across the three cell lines prompted us to examine alternative intracellular proteolytic activities. Calpains are another class of cysteine proteases that parallel caspases in cell death models with increased activities observed during necrotic as well as apoptotic cell death [27]. Increases in calpain activity were monitored by the hydrolysis of specific fluorogenic calpain substrate (Suc-LLVY-AMC) after treatment of all three cell lines with 250 μM TFEC for 0–8 h. As shown in Fig. 8, a progressive increase in calpain activity was observed with TAMH-Vc cells, which peaked at 6 h treatment with absolute activity of 86.5 ± 8.1 *p*mol hydrolyzed product/h. This indicates an approximate 2-fold increase in basal calpain activity ($P < 0.05$). On the other hand, the activation seen in BCL-xL cells in comparison were insignificant at 0–6 h ($P < 0.05$) with a modest increase at 8 h (i.e., 69.5 ± 9.3) ($P < 0.05$). Statistically significant difference was also confirmed between the two cells lines using an unpaired *t*-test at early time points of TFEC treatment (i.e., 2 and 4 h; $P < 0.05$), indicating either a delayed response or attenuation of calpain activation in TAMH-BCL-xL cells. Specificity of this assay was determined by reversal of calpain-mediated hydrolysis using the calpain inhibitors ALLM

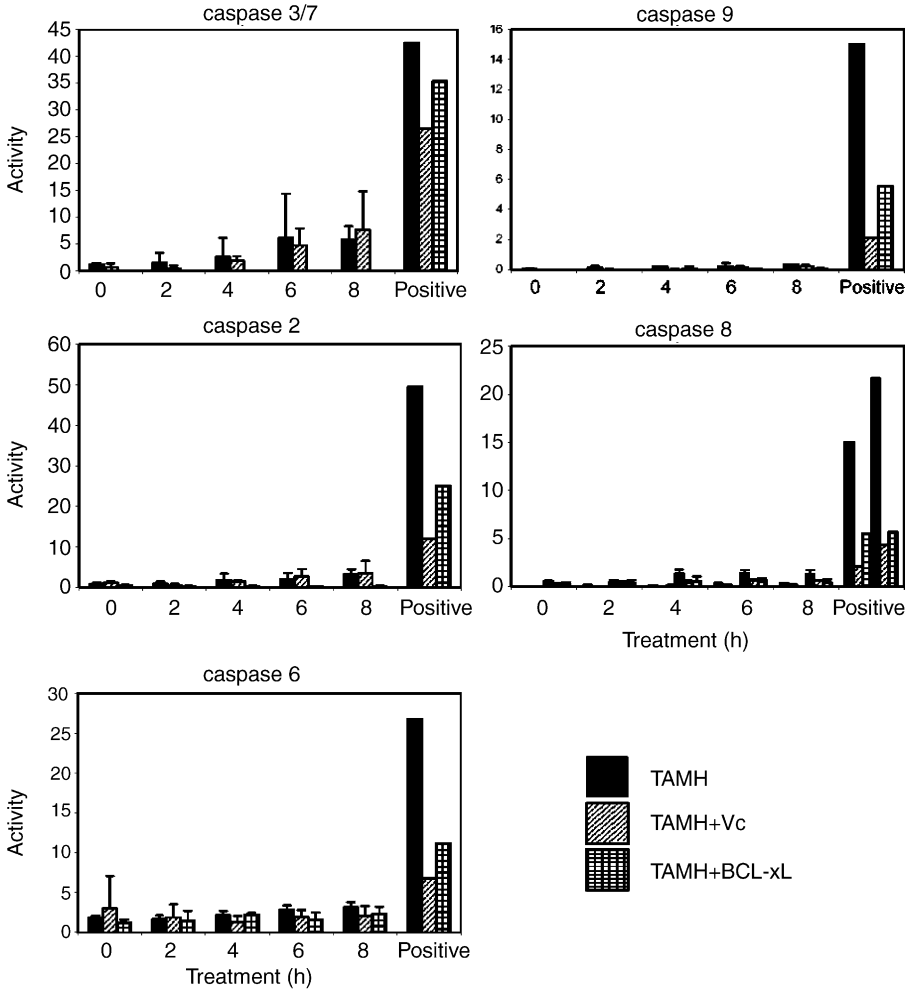

Fig. 7. Caspase activity assays for TFEC treated TAMH, TAMH-Vc and TAMH-BCL-xL cells: cells were treated with 250 mM of TFEC for 2, 4, 6 and 8 h. Caspase activities were quantified by the amount of specific fluorogenic caspase-substrates hydrolyzed (*p*mol of AMC substrates) per μg total lysate protein per minute of incubation for the assay with ±S.E.M. ($n = 3$). These values were compared against an actinomycin-D/TNF-α treated positive control for 8 h. The substrates used were (A) Ac-DEVD-AMC for caspase-3/7; (B) Ac-VDVAD-AMC for caspase-2; (C) Ac-VEID-AMC for caspase-6; (D) Ac-IETD-AMC for caspase-8; and (E) Ac-LEHD-AMC for caspase-9.

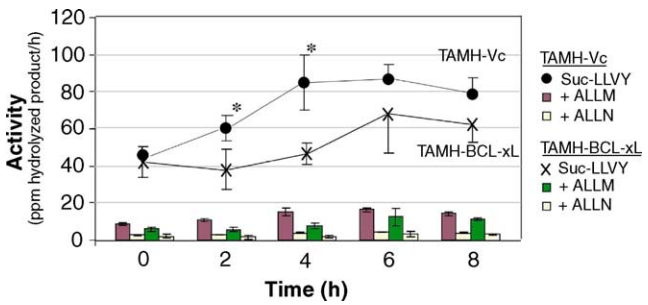

Fig. 8. Calpain activity assays for TFEC treated TAMH-Vc and TAMH-BCL-xL cells: cells were treated with 250 mM of TFEC for 2, 4, 6 and 8 h. Calpain activity was quantified by the amount of specific fluorogenic calpain substrate hydrolyzed (*p*mol of Suc-LLVY-AMC) per μg total lysate protein per minute of incubation for the assay with ±S.E.M. ($n = 3$). Specific calpain inhibitors, ALLM and ALLM were co-administered in parallel experiments to demonstrate the selectivity of the activation. (* indicates a statistically significant difference between the two cell lines as determined by unpaired *t*-test, $P < 0.05$).

and ALLN. A 100 μM inhibitor concentration decreased calpain activity to less than 20% of the non-inhibitor treated samples, suggesting that TFEC preferentially activates calpains compared to caspases in the TAMH cell line.

4. Discussion

In recent years, several studies in molecular toxicology have focused on BCL-2 proteins as central to the early events of drug-induced cytotoxicity. Amongst them, pro-apoptotic BAX is probably one of the best-studied members. BAX is known to be constitutively expressed in the cytosol and found to relocate to the mitochondrial membrane upon induction of cellular injury from many different origins [28–30]. It represents an important early factor, which initiates downstream mitochondrial changes thereby

predisposing to apoptosis. Although the precise mechanism(s) of BAX activation and function are not yet known, there are different schools of thought as to how this subcellular migration confers a pro-apoptotic character. Some studies have reported that BAX enables the release of several effectors of apoptosis like AIF, cytochrome *c*, and SMAC/DIABLO by creating a channel in the mitochondrial membrane [31]. Others have provided evidence for homodimerization and oligomerization [23,32] with other anti-apoptotic members like BCL-xL to inhibit the latter's cytoprotective actions [33–35]. In general agreement with these studies, our immunoblot and immunocytochemical studies also suggest that BAX translocation is an early event in TFEC-induced cytotoxicity with significant BAX relocation at 2 h or earlier after treatment with TFEC (Fig. 1).

We have also observed that although native BAX resides in the cytosol, a small amount may be constitutively present in the outer mitochondrial membrane in agreement with other studies (Figs. 1 and 2) [36]. The functional significance of this constitutive mitochondrial BAX is not yet known. As previously proposed, it could imply that an equilibrium exists between the pro-apoptotic and anti-apoptotic BCL-2 proteins such that when BAX is in excess, some can be distributed to the mitochondrial membrane [34,37]. This appears to be supported by our data with the BCL-xL overexpressed TAMH cell line, which has a significantly lower content of BAX in the mitochondria at rest, even though the overall expression level of BAX has not been altered (Figs. 1 and 2).

Numerous reports confirm a role for anti-apoptotic BCL-2 members in inhibiting pro-apoptotic BAX activation, notably at the level of its translocation to the mitochondria [38–40]. These studies underlie the known role of BCL-xL as a dominant anti-apoptotic player in the BCL-2 family. In particular, it has been reported that BCL-xL, but not BCL-2, is the major BCL-2 homologous anti-apoptotic protein in hepatocytes [14,15]. As a result, our studies differ from previous work in that we have investigated the effects of overexpression of the tissue appropriate BCL-2 family member in the TAMH cell line. Interestingly, our previous work has raised paradoxical questions regarding the tissue inappropriate overexpression of BCL-2 per se in the liver with a failure to protect against BAX-mediated, acetaminophen-induced hepatotoxicity [41]. These previous observations suggest that BCL-2 family members have non-redundant and tissue-specific functions, which can include either anti- or pro-apoptotic activities.

Although we have demonstrated here that TFEC treatment has resulted in an increased activated BAX expression and translocation, we have also examined other downstream markers in order to show that this change in BAX activity is ultimately translated into a measurable cytotoxicity endpoint. Thus, we have confirmed by immunoblot that cytochrome *c*—a potential effector of BAX activation—was released from the intramitochondrial membrane spaces into the cytosol over a period of 8 h with TFEC treatment. Furthermore, our results also indicated a time delay between BAX translocation and cytochrome *c* release, supporting the proposition that BAX translocation is, at least in part, required for cytochrome *c* release during TFEC-induced cytotoxicity.

Cytochrome *c* release is recognized as instrumental in the formation of the activated apoptosome complex, which is central to caspase activation and most forms of apoptosis. In the present work, however, only limited caspase activation was observed following TFEC treatment despite cytochrome *c* leakage. On the other hand, we detected a strong activation of an alternative cysteine protease, calpain, which was also inhibitable by BCL-xL overexpression. Calpain activation is driven by intracellular calcium mobilization and its proteolytic activities can proceed in an ATP-independent fashion. Our findings confirm previous preliminary reports of a role for calpain [42]. Thus, these results, in addition to prior morphological evidence, would appear to support necrosis as the dominant pathway for TFEC-mediated cytotoxicity [6]. Nonetheless, the observations presented here implicate an early role for pro-apoptotic BAX in this form of cell death.

Although not examined directly in these studies, it is likely that the covalent modification of intramitochondrial targets by TFEC could also initiate intracellular stress signaling pathways (e.g., JNK), which facilitate the early mitochondrial manifestation of apoptosis. Previously, we have shown that such intramitochondrial protein modifications inhibit rate-limiting steps in the TCA cycle [5]. As a result, cellular ATP levels would be expected to undergo rapid depletion and this, in turn, may shift the mechanism of cell death from apoptosis to secondary necrosis (Ho et al., in preparation).

HSP70i induction was used in these studies as an indicator of TFEC-induced protein damage in exposed TAMH cultures (Fig. 6). Increased cytoprotective BCL-xL levels were associated with absence of HSP70i induction following TFEC treatment in contrast to ATF3, which was unaffected. These findings are consistent with the prominent roles that the HSP70 family plays in the recognition of protein native state. In particular, the highly inducible HSP70i isoform is known to confer cytoprotective effects in response to many stressors by limiting excessive protein aggregation and misfolding [43,44]. An alternative term ''proteotoxicity'', first coined by Hightower in 1991, adequately describes such loss of protein homeostasis [45]. The literature also defines additional roles for HSP70i including inhibition of specific apoptotic steps such as JNK activation and apoptosome complex formation [44,46]. Furthermore, it has been shown that the amount of HSP70i induction correlates with the ultimate extent of cytoprotection [47,48]. Elevated HSP70i levels in our studies are viewed

as indicative of TFEC-mediated proteotoxicity in both TAMH and TAMH-Vc cultures. Therefore, the most likely interpretation for the lack of HSP70i upregulation in BCL-xL overexpressing cells is a reduction in proteotoxic damage caused by TFEC (Fig. 6). Nonetheless, further work is required to provide a direct mechanistic link between BCL-xL overexpression and HSP70i regulation. Of relevance, similar observations have also been reported with BCL-xL-mediated protection from heat shock [49].

Analogous to our findings with HSP70i, we also report increased levels of expression of stress-responsive ATF3 following TFEC treatment of TAMH cells (both with and without BCL-xL overexpression). ATF3 belongs to a family of transcription factors that contain the basic region-leucine zipper (bZip) DNA binding domain [26]. Induction of the *atf3* gene appears as an early response to several forms of cellular stress, including liver dysfunction [50]. In addition to the immunoblot analyses presented here, we have also confirmed increased transcriptional upregulation of the *atf3* gene in TAMH cells after TFEC treatment by both cDNA microarray analyses and quantitative RT-PCR (Hu et al., in preparation). Since BCL-xL overexpression does not directly alter the expression of TFEC-induced ATF3 upregulation, the observed cytoprotective effects of BCL-xL may be downstream from ATF3, or through a mechanism that is independent of the ATF3-mediated stress response. More recently, studies have revealed that ATF3 serves an integral role in the ER stress response [51,52]. In independent investigations, we have also confirmed the transcriptional (*gadd153*, *gadd34*, *gadd45*) and translational (*gadd153*) upregulation of some established ATF3-regulated ER dependent stress response genes (Hu et al., in preparation). Taken together, these findings suggest an early ER stress response associated with TFEC-induced mitochondrial events that may not be inhibited by BCL-xL overexpression. Further investigation of the interrelationship of these two proteins will be necessary to address these questions.

The effects of BCL-xL on TFEC-treated TAMH cells extend beyond a modulation of early events of cell death as exemplified by BAX translocation, HSP70i induction and cytochrome *c* release. Our results have also revealed that BCL-xL overexpression in this model system has an important and reproducible function in determining the overall level of cell survival to chemical insult. TAMH-BCL-xL cells were less susceptible to TFEC-induced cell death as compared to both the parental TAMH and the TAMH-Vc cell lines. The possibility remains that this cytoprotective effect of BCL-xL on chemically mediated necrotic damage may translate into an effective chemo-preventative therapeutic strategy.

In summary, a cytoprotective action of BCL-xL on BAX-mediated toxicity has been demonstrated in TFEC-induced cell death. Although, there is insufficient information to conclude either a direct interaction between BCL-xL and BAX, or an indirect modulation [53], BCL-xL has previously been reported to form heterodimers with BAX to limit the pro-apoptotic actions of the latter [33,34,39]. In conclusion, BAX activation appears as an early event in TFEC-induced cell death and our findings could open new avenues for BCL-xL mimetics in the treatment of adverse effects from other compounds, previously considered necrotic in mechanism, but similarly acting through a BAX pathway.

Acknowledgements

This work was supported by NIH grants GM51916 (SB), GM32165 (SDN), CA74131 (NF), UW NIEHS sponsored Center for Ecogenetics and Environmental Health: NIEHS P30ES07033 and American Cancer Society RPG-00-222-01-CDD (DMH). We would also like to express our gratitude to Greg Martin for his assistance with fluorescent microscopy, Chris Franklin for helpful discussion and guidance on caspase activity assays and Catherine Le for immunocytochemical assays.

References

[1] Krahenbuhl S. Mitochondria: important target for drug toxicity? J Hepatol 2001;34:334–6.
[2] Ravagnan L, Roumier T, Kroemer G. Mitochondria, the killer organelles and their weapons. J Cell Physiol 2002;192:131–7.
[3] Lock EA, Ishmael J. The nephrotoxicity and hepatotoxicity of 1,1,2,2-tetrafluoroethyl-L-cysteine in the rat. Arch Toxicol 1998;72:347–54.
[4] Cooper AJ, Bruschi SA, Anders MW. Toxic, halogenated cysteine S-conjugates and targeting of mitochondrial enzymes of energy metabolism. Biochem Pharmacol 2002;64:553–64.
[5] James EA, Gygi SP, Adams ML, Pierce RH, Fausto N, Aebersold RH, et al. Mitochondrial aconitase modification, functional inhibition, and evidence for a supramolecular complex of the TCA cycle by the renal toxicant S-(1,1,2,2-tetrafluoroethyl)-L-cysteine. Biochemistry 2002;41:6789–97.
[6] Bruschi SA, Lindsay JG, Crabb JW. Mitochondrial stress protein recognition of inactivated dehydrogenases during mammalian cell death. Proc Natl Acad Sci U S A 1998;95:13413–8.
[7] Bruschi SA, West KA, Crabb JW, Gupta RS, Stevens JL. Mitochondrial HSP60 (P1 protein) and a HSP70-like protein (mortalin) are major targets for modification during S-(1,1,2,2-tetrafluoroethyl)-L-cysteine-induced nephrotoxicity. J Biol Chem 1993;268:23157–61.
[8] Zhan Y, van de Water B, Wang Y, Stevens JL. The roles of caspase-3 and bcl-2 in chemically-induced apoptosis but not necrosis of renal epithelial cells. Oncogene 1999;18:6505–12.
[9] Groves CE, Hayden PJ, Lock EA, Schnellmann RG. Differential cellular effects in the toxicity of haloalkene and haloalkane cysteine conjugates to rabbit renal proximal tubules. J Biochem Toxicol 1993;8:49–56.
[10] Groves CE, Lock EA, Schnellmann RG. Role of lipid peroxidation in renal proximal tubule cell death induced by haloalkene cysteine conjugates. Toxicol Appl Pharmacol 1991;107:54–62.
[11] Wu JC, Merlino G, Cveklova K, Mosinger Jr B, Fausto N. Autonomous growth in serum-free medium and production of hepatocellular carcinomas by differentiated hepatocyte lines that overexpress transforming growth factor alpha 1. Cancer Res 1994;54:5964–73.

[12] Pierce RH, Campbell JS, Stephenson AB, Franklin CC, Chaisson M, Poot M, et al. Disruption of redox homeostasis in tumor necrosis factor-induced apoptosis in a murine hepatocyte cell line. Am J Pathol 2000;157:221–36.
[13] Pierce RH, Franklin CC, Campbell JS, Tonge RP, Chen W, Fausto N, et al. Cell culture model for acetaminophen-induced hepatocyte death in vivo. Biochem Pharmacol 2002;64:413–24.
[14] Takehara T, Liu X, Fujimoto J, Friedman SL, Takahashi H. Expression and role of Bcl-xL in human hepatocellular carcinomas. Hepatology 2001;34:55–61.
[15] Tzung SP, Fausto N, Hockenbery DM. Expression of Bcl-2 family during liver regeneration and identification of Bcl-x as a delayed early response gene. Am J Pathol 1997;150:1985–95.
[16] Gross A, McDonnell JM, Korsmeyer SJ. BCL-2 family members and the mitochondria in apoptosis. Genes Dev 1999;13:1899–911.
[17] Tzung SP, Kim KM, Basanez G, Giedt CD, Simon J, Zimmerberg J, et al. Antimycin A mimics a cell-death-inducing Bcl-2 homology domain 3. Nat Cell Biol 2001;3:183–91.
[18] Single B, Leist M, Nicotera P. Simultaneous release of adenylate kinase and cytochrome *c* in cell death. Cell Death Differ 1998;5: 1001–3.
[19] Dietze EC, Schafer A, Omichinski JG, Nelson SD. Inactivation of glyceraldehyde-3-phosphate dehydrogenase by a reactive metabolite of acetaminophen and mass spectral characterization of an arylated active site peptide. Chem Res Toxicol 1997;10:1097–103.
[20] Plumb JA, Milroy R, Kaye SB. Effects of the pH dependence of 3-(4,5-dimethylthiazol-2-yl)-2,5-diphenyl-tetrazolium bromide-formazan absorption on chemosensitivity determined by a novel tetrazolium-based assay. Cancer Res 1989;49:4435–40.
[21] Decker T, Lohmann-Matthes ML. A quick and simple method for the quantitation of lactate dehydrogenase release in measurements of cellular cytotoxicity and tumor necrosis factor (TNF) activity. J Immunol Methods 1988;115:61–9.
[22] Mikhailov V, Mikhailova M, Degenhardt K, Venkatachalam MA, White E, Saikumar P. Association of Bax and Bak homo-oligomers in mitochondria. Bax requirement for Bak reorganization and cytochrome *c* release. J Biol Chem 2003;278:5367–76.
[23] Mikhailov V, Mikhailova M, Pulkrabek DJ, Dong Z, Venkatachalam MA, Saikumar P. Bcl-2 prevents Bax oligomerization in the mitochondrial outer membrane. J Biol Chem 2001;276:18361–74.
[24] Kregel KC. Heat shock proteins: modifying factors in physiological stress responses and acquired thermotolerance. J Appl Physiol 2002;92:2177–86.
[25] Zhang C, Gao C, Kawauchi J, Hashimoto Y, Tsuchida N, Kitajima S. Transcriptional activation of the human stress-inducible transcriptional repressor ATF3 gene promoter by p53. Biochem Biophys Res Commun 2002;297:1302–10.
[26] Hai T, Wolfgang CD, Marsee DK, Allen AE, Sivaprasad U. ATF3 and stress responses. Gene Expr 1999;7:321–35.
[27] Wang KK. Calpain and caspase: can you tell the difference? Trends Neurosci 2000;23:20–6.
[28] Zhang H, Heim J, Meyhack B. Redistribution of Bax from cytosol to membranes is induced by apoptotic stimuli and is an early step in the apoptotic pathway. Biochem Biophys Res Commun 1998;251:454–9.
[29] Wolter KG, Hsu YT, Smith CL, Nechushtan A, Xi XG, Youle RJ. Movement of Bax from the cytosol to mitochondria during apoptosis. J Cell Biol 1997;139:1281–92.
[30] Hsu YT, Wolter KG, Youle RJ. Cytosol-to-membrane redistribution of Bax and Bcl-X(L) during apoptosis. Proc Natl Acad Sci U S A 1997;94:3668–72.
[31] Eskes R, Desagher S, Antonsson B, Martinou JC. Bid induces the oligomerization and insertion of Bax into the outer mitochondrial membrane. Mol Cell Biol 2000;20:929–35.
[32] Antonsson B, Montessuit S, Sanchez B, Martinou JC. Bax is present as a high molecular weight oligomer/complex in the mitochondrial membrane of apoptotic cells. J Biol Chem 2001;276:11615–23.
[33] Antonawich FJ, Krajewski S, Reed JC, Davis JN. Bcl-x(l) Bax interaction after transient global ischemia. J Cereb Blood Flow Metab 1998;18:882–6.
[34] Oltvai ZN, Milliman CL, Korsmeyer SJ. Bcl-2 heterodimerizes in vivo with a conserved homolog, Bax, that accelerates programmed cell death. Cell 1993;74:609–19.
[35] Shangary S, Johnson DE. Peptides derived from BH3 domains of Bcl-2 family members: a comparative analysis of inhibition of Bcl-2, Bcl-x(L) and Bax oligomerization, induction of cytochrome *c* release, and activation of cell death. Biochemistry 2002;41:9485–95.
[36] Putcha GV, Deshmukh M, Johnson Jr EM. BAX translocation is a critical event in neuronal apoptosis: regulation by neuroprotectants, BCL-2, and caspases. J Neurosci 1999;19:7476–85.
[37] Chao DT, Korsmeyer SJ. BCL-2 family: regulators of cell death. Annu Rev Immunol 1998;16:395–419.
[38] Murphy KM, Ranganathan V, Farnsworth ML, Kavallaris M, Lock RB. Bcl-2 inhibits Bax translocation from cytosol to mitochondria during drug-induced apoptosis of human tumor cells. Cell Death Differ 2000;7:102–11.
[39] Ganju N, Eastman A. Bcl-X(L) and calyculin A prevent translocation of Bax to mitochondria during apoptosis. Biochem Biophys Res Commun 2002;291:1258–64.
[40] Finucane DM, Bossy-Wetzel E, Waterhouse NJ, Cotter TG, Green DR. Bax-induced caspase activation and apoptosis via cytochrome *c* release from mitochondria is inhibitable by Bcl-xL. J Biol Chem 1999;274:2225–33.
[41] Adams ML, Pierce RH, Vail ME, White CC, Tonge RP, Kavanagh TJ, et al. Enhanced acetaminophen hepatotoxicity in transgenic mice overexpressing BCL-2. Mol Pharmacol 2001;60:907–15.
[42] Schnellmann RG, Williams SW. Proteases in renal cell death: calpains mediate cell death produced by diverse toxicants. Ren Fail 1998;20: 679–86.
[43] Kabakov AE, Budagova KR, Latchman DS, Kampinga HH. Stressful preconditioning and HSP70 overexpression attenuate proteotoxicity of cellular ATP depletion. Am J Physiol Cell Physiol 2002;283: C521–34.
[44] Beere HM, Green DR. Stress management–heat shock protein-70 and the regulation of apoptosis. Trends Cell Biol 2001;11:6–10.
[45] Hightower LE. Heat shock, stress proteins, chaperones, and proteotoxicity. Cell 1991;66:191–7.
[46] Salminen Jr WF, Voellmy R, Roberts SM. Protection against hepatotoxicity by a single dose of amphetamine: the potential role of heat shock protein induction. Toxicol Appl Pharmacol 1997;147:247–58.
[47] Van Molle W, Wielockx B, Mahieu T, Takada M, Taniguchi T, Sekikawa K, et al. HSP70 protects against TNF-induced lethal inflammatory shock. Immunity 2002;16:685–95.
[48] Mosser DD, Caron AW, Bourget L, Denis-Larose C, Massie B. Role of the human heat shock protein hsp70 in protection against stress-induced apoptosis. Mol Cell Biol 1997;17:5317–27.
[49] Robertson JD, Datta K, Kehrer JP. Bcl-xL overexpression restricts heat-induced apoptosis and influences hsp70, bcl-2, and Bax protein levels in FL5.12 cells. Biochem Biophys Res Commun 1997;241: 164–8.
[50] Allen-Jennings AE, Hartman MG, Kociba GJ, Hai T. The roles of ATF3 in liver dysfunction and the regulation of phosphoenolpyruvate carboxykinase gene expression. J Biol Chem 2002;277:20020–5.
[51] Jiang HY, Wek SA, McGrath BC, Lu D, Hai T, Harding HP, et al. Activating transcription factor 3 is integral to the eukaryotic initiation factor 2 kinase stress response. Mol Cell Biol 2004;24:1365–77.
[52] Zhang C, Kawauchi J, Adachi MT, Hashimoto Y, Oshiro S, Aso T, et al. Activation of JNK and transcriptional repressor ATF3/LRF1 through the IRE1/TRAF2 pathway is implicated in human vascular endothelial cell death by homocysteine. Biochem Biophys Res Commun 2001;289:718–24.
[53] Pan G, O'Rourke K, Dixit VM. Caspase-9, Bcl-XL, and Apaf-1 form a ternary complex. J Biol Chem 1998;273:5841–5.